

# 无机化学学报

2017 年

第 33 卷

第 3 期

## 目 次

### 综 述

镧系离子掺杂的近红外复合光催化剂的合成研究进展

.....李耀武 黄辰曦 陶 伟 钱海生(361)

### 论 文

锂离子电池 Si/RGO@PANI 三明治纳米结构负极材料的制备与电化学性能

.....张兴帅 许笑目 郭玉忠 黄瑞安 王剑华 杨 斌 戴永年(377)

磁性壳聚糖复合微球的制备及其  $\text{Cu}^{2+}$  吸附性能

.....李建军 鲍 旭 吴先锋 Islam Nazrul 刘 银 乔尚元 余臻伟 朱金波(383)

$\text{MoS}_2/\text{g-C}_3\text{N}_4$  复合材料的制备及可见光催化性能

.....徐梦秋 柴 波 闫俊涛 汪海波 任占冬(389)

中空花状可见光响应催化剂  $\text{g-C}_3\text{N}_4/\text{BiOCl}$  的制备及其光催化活性

.....杨冰叶 李 航 商宁昭 冯 成 高书涛 王 春(396)

以 2,3-二苯基吡嗪或 2,3-二苯基喹喔啉为配体的单核和双核金属铂配合物的晶体结构与光物理性质

.....骆开均 耿 浩 张晨阳 倪海亮 李 权(405)

$\text{Pd-Al}_2\text{O}_3\text{-BEA}$  催化剂催化油脂一步加氢制航空燃油烃类性能

.....杜君臣 张爱敏 马江丽 刘 强 冯 丰 陈玉保 赵云昆(415)

非晶态  $\text{ZrO}_2$  镶嵌的超细  $\text{CeO}_2$  催化  $\text{HCl}$  氧化

.....徐希化 楼家伟 谢兴星 费兆阳 刘 清 陈 献 汤吉海 崔咪芬 乔 旭(421)

锂离子电池  $\text{LiTi}_{0.25}\text{Fe}_{0.75}\text{SO}_4\text{F}$  正极材料的电子结构.....陶 伟 黄 云 伊廷锋 谢 颖(429)

Sb 掺杂 ZTO 透明导电薄膜的结构和性能.....陈 肖 李一鸣 刘晓军 贺蕴秋(435)

pH 值响应性毒死蜱/铜席夫碱配合物改性 SBA-15 的制备及缓释性能

.....林粤顺 周红军 周新华 龚 圣 徐 华 陈铎耀(446)

球形  $\text{Bi}_4\text{Ti}_3\text{O}_{12}$  制备及其可见光催化性能.....高晓明 代 源 张 裕 王子航 付 峰(455)

氨基喹啉水杨醛 Schiff 碱配合物的合成、晶体结构及抑菌性能

.....史 娟 李 江 葛红光(463)

三维有序大孔  $\text{Fe}_2\text{SiO}_4/\text{SiO}_2/\text{C}$  锂离子电池负极纳米玻璃陶瓷-碳复合材料制备及电化学性能

.....孙 茹 李东林 陈光琦 张 巍 樊小勇 苟 蕾 王艳茹 程旖旎 赵珍珍(471)

多孔微纳结构富锂正极材料  $0.6\text{Li}_2\text{MnO}_3 \cdot 0.4\text{LiNi}_{0.5}\text{Mn}_{0.5}\text{O}_2$  的制备及其电化学性能

.....郑 卓 吴振国 向 伟 杨秀山(479)

半夹芯式 16 电子化合物  $\text{CpCo}(\text{S}_2\text{C}_2\text{B}_{10}\text{H}_{10})$  与重氮乙酸乙酯及联烯三元反应体系

.....刘贵锋 燕 红(487)

铈酸锰-还原氧化石墨烯复合光催化剂的构建以及可见光下降解亚甲基蓝(英文)	顾巍 严铭 孙林 施伟东(493)
氮化钛纳米管作为钒电池负极对 V(II)/V(III)的电化学性能(英文)	赵峰鸣 闻刚 孔丽瑶 褚有群 马淳安(501)
ZnO/BiOI 微球的合成及其光催化性能(英文)	王元有 龚爱琴 余文华(509)
Ag <sub>2</sub> CO <sub>3</sub> /BiVO <sub>4</sub> 复合微米片光催化剂的制备、表征及光催化机理	刘仁月 吴榛 白羽 余长林 李家德 舒庆 杨凯(519)
《无机化学学报》投稿须知(NOTICE TO AUTHORS)	(528)

# CHINESE JOURNAL OF INORGANIC CHEMISTRY

Vol.33

No.3

Mar. 2017

## CONTENTS

### Cover



#### Synthetic Progress of Compositd Photocatalysts Doped by Lanthanide Ions and Driven by Near Infrared Light

LI Yao-Wu, HUANG Chen-Xi, TAO Wei, QIAN Hai-Sheng

DOI:10.11862/CJIC.2017.038

*Chinese J. Inorg. Chem.*, **2017**,33:361-376

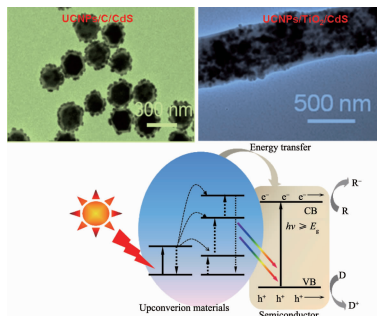
### Reviews

#### Synthetic Progress of Compositd Photocatalysts Doped by Lanthanide Ions and Driven by Near Infrared Light

LI Yao-Wu, HUANG Chen-Xi, TAO Wei, QIAN Hai-Sheng

DOI:10.11862/CJIC.2017.038

*Chinese J. Inorg. Chem.*, **2017**,33:361-376



Energy crisis and environmental pollution have attracted seriously worldwide attention. The lanthanide ions doped upconversion nanostructures/semiconductors composite photocatalysts have attracted much attention. The synthetic techniques for fabrication of the composited photocatalysts, including epitaxial growth, electrospinning, chemical assembly and so on, have been highlighted for wastewater treatment and water splitting triggered by near infrared light.

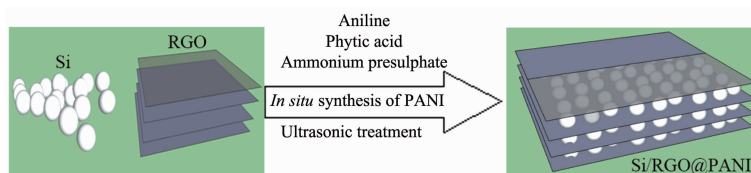
### Articles

#### Preparation and Electrochemical Properties of Sandwich-like Si/RGO@PANI Nanocomposite as Anode for Lithium Ion Battery

ZHANG Xing-Shuai, XU Xiao-Mu, GUO Yu-Zhong, HUANG Rui-An, WANG Jian-Hua, YANG Bin, DAI Yong-Nian

DOI:10.11862/CJIC.2017.057

*Chinese J. Inorg. Chem.*, **2017**,33:377-382



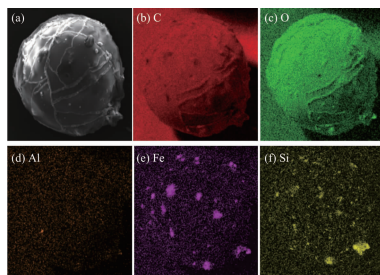
A sandwich-like Si/RGO@PANI nanocomposite consisting of RGO, PANI and nano Si particles reveals very good conductivity and can endure the great volume change of silicon during Li-ion insertion/extraction processes. Thus, this nanocomposite exhibits excellent electrochemical performance as a Li-ion battery anode material.

## Magnetic Chitosan Micron Spheres: Synthesis and Adsorption Property for $\text{Cu}^{2+}$

LI Jian-Jun, BAO Xu, WU Xian-Feng,  
Islam Nazrul, LIU Yin, QIAO Shang-Yuan,  
YU Zhen-Wei, ZHU Jin-Bo

DOI:10.11862/CJIC.2017.052

*Chinese J. Inorg. Chem.*, **2017**,**33**:383-388



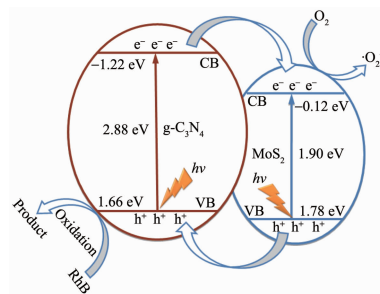
Coal-fly-ash magnetic spheres (MS) were employed as magnetic core to fabricate  $\text{MS@SiO}_2\text{@Chitosan}$  magnetic microspheres. The obtained micro-spheres exhibited a much higher  $\text{Cu}^{2+}$  adsorbability compared with the original coal-fly-ash magnetic spheres. And they could be separated effectively from water by magnetic separation.

## Synthesis and Visible Light Photocatalytic Performance of $\text{MoS}_2/\text{g-C}_3\text{N}_4$ Composites

XU Meng-Qiu, CHAI Bo, YAN Jun-Tao,  
WANG Hai-Bo, REN Zhan-Dong

DOI:10.11862/CJIC.2017.045

*Chinese J. Inorg. Chem.*, **2017**,**33**:389-395



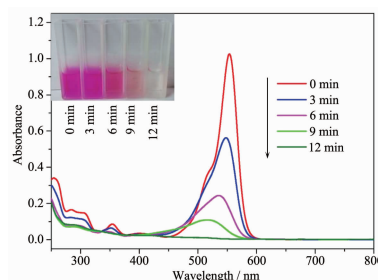
The  $\text{MoS}_2/\text{g-C}_3\text{N}_4$  composites with significantly enhanced visible light photocatalytic performances were fabricated through combining the exfoliated commercial  $\text{MoS}_2$  with  $\text{g-C}_3\text{N}_4$ .

## Visible-Light Responsive Photocatalyst $\text{g-C}_3\text{N}_4\text{@BiOCl}$ with Hollow Flower-like Structure: Preparation and Photocatalytic Performance

YANG Bing-Ye, LI Hang, SHANG Ning-Zhao,  
FENG Cheng, GAO Shu-Tao, WANG Chun

DOI:10.11862/CJIC.2017.033

*Chinese J. Inorg. Chem.*, **2017**,**33**:396-404



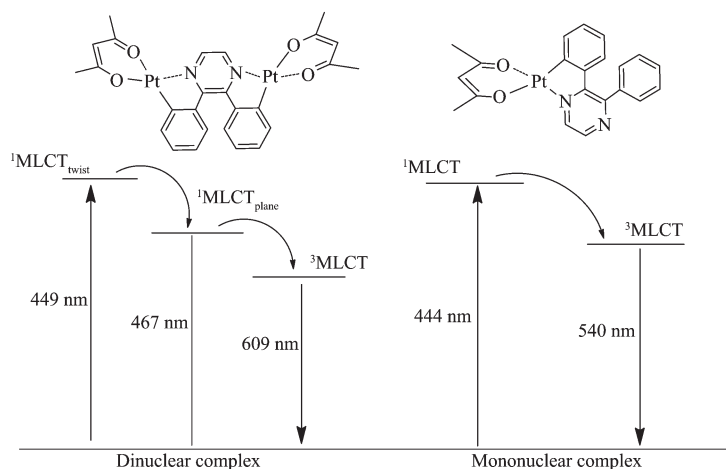
The heterojunction photocatalyst of  $\text{g-C}_3\text{N}_4\text{@BiOCl}$  with hollow flower-like structure was fabricated and exhibited much higher photocatalytic activity than  $\text{g-C}_3\text{N}_4$  and  $\text{BiOCl}$  under visible-light irradiation ( $\lambda \geq 420 \text{ nm}$ ). The degradation efficiency of  $50 \text{ mg} \cdot \text{L}^{-1}$  rhodamine B can be reached to 99% within 12 min.

## Mononuclear and Dinuclear Platinum(II) Complexes Based on Bridging Ligands 2,3-Diphenylpyrazine or 2,3-Diphenylquinoxaline: Crystal Structures and Photophysical Properties

LUO Kai-Jun, GENG Hao,  
ZHANG Cheng-Yang, NI Hai-Liang, LI Quan

DOI:10.11862/CJIC.2017.026

*Chinese J. Inorg. Chem.*, **2017**,**33**:405-414

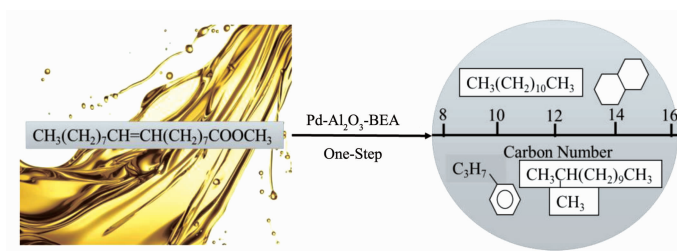


Pd-Al<sub>2</sub>O<sub>3</sub>-BEA Catalysts for the Preparation of Jet Fuel-Range Hydrocarbons from Oils Through One-Step Hydrogenation

DU Jun-Chen, ZHANG Ai-Min, MA Jiang-Li, LIU Qiang, FENG Feng, CHEN Yu-Bao, ZHAO Yun-Kun

DOI:10.11862/CJIC.2017.027

*Chinese J. Inorg. Chem.*, **2017**,**33**:415-420



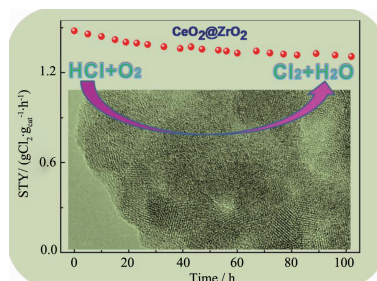
H- $\beta$  modified Pd/Al<sub>2</sub>O<sub>3</sub> material with appropriate pore distribution and acidity has been investigated as an efficient catalyst for the preparation of jet fuel-range hydrocarbons from oils by one-step hydrogenation reaction.

Superfine CeO<sub>2</sub> Embedded in a Porous ZrO<sub>2</sub> Matrix for Catalytic HCl Oxidation

XU Xi-Hua, LOU Jia-Wei, XIE Xing-Xing, FEI Zhao-Yang, LIU Qing, CHEN Xian, TANG Ji-Hai, CUI Mi-Fen, QIAO Xu

DOI:10.11862/CJIC.2017.047

*Chinese J. Inorg. Chem.*, **2017**,**33**:421-428



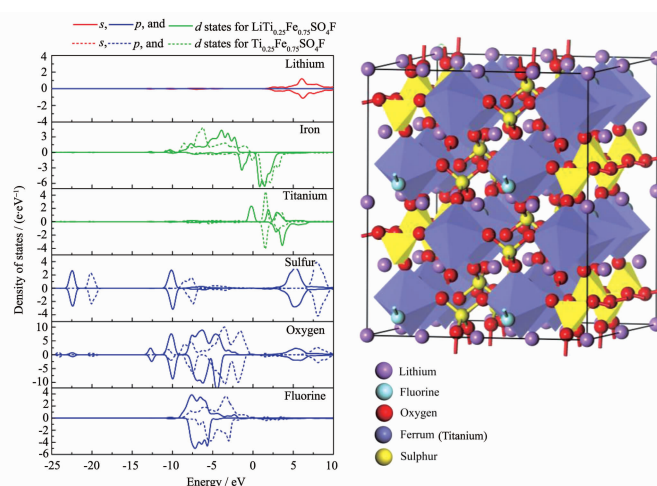
Nano-sized CeO<sub>2</sub> particles embedded in the amorphous ZrO<sub>2</sub> matrix for recycling of Cl<sub>2</sub> from HCl oxidation, which are thus prevented from sintering during the reaction.

Electronic Structure of LiTi<sub>0.25</sub>Fe<sub>0.75</sub>SO<sub>4</sub>F Positive-Electrode Material for Lithium-Ion Battery

TAO Wei, HUANG Yun, YI Ting-Feng, XIE Ying

DOI:10.11862/CJIC.2017.043

*Chinese J. Inorg. Chem.*, **2017**,**33**:429-434



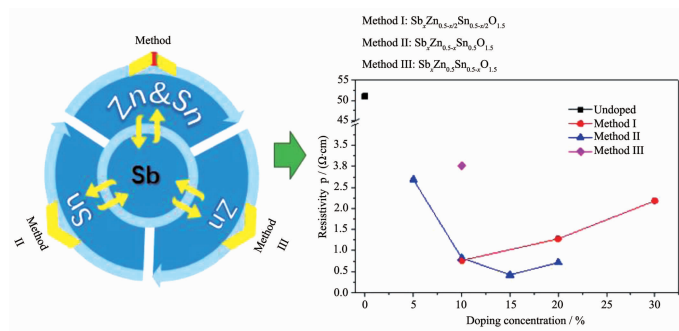
Ti doping results in the disappearance of the band gap, and then significantly enhances the electric conductivity and structural stability of LiFeSO<sub>4</sub>F cathode materials.

## Structures and Properties of Sb-Doped ZTO Transparent Conducting Films

CHEN Xiao, LI Yi-Ming, LIU Xiao-Jun,  
HE Yun-Qiu

DOI:10.11862/CJIC.2017.039

*Chinese J. Inorg. Chem.*, **2017**,**33**:435-445



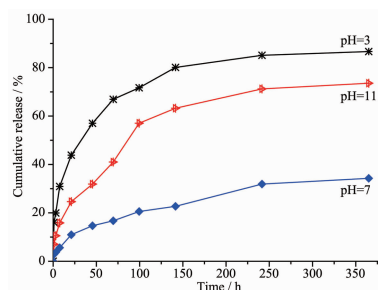
By the three substitution methods (I, II and III), the Sb ions successfully entered into the lattice positions of the target ions as designed, resulting in the variation of the conductivity of the Sb-doped ZTO films.

## Preparation and Properties of pH Value-Responsive Sustained Release System of Chlorpyrifos/Copper(II) Schiff Base SBA-15

LIN Yue-Shun, ZHOU Hong-Jun,  
ZHOU Xin-Hua, GONG Sheng, XU Hua,  
CHEN Hua-Yao

DOI:10.11862/CJIC.2017.056

*Chinese J. Inorg. Chem.*, **2017**,**33**:446-454



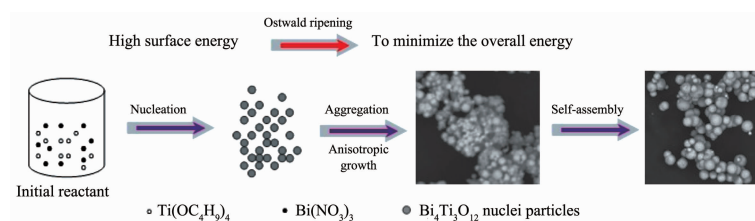
The chlorpyrifos/copper Schiff base modified SBA-15 (CH-Cu-SBA-15) sustained release system showed significant sensitivity in response to the pH value, which was of potential value for agricultural control of pests and diseases. Meanwhile, their releasing curves could be described by Riger-Peppas equation.

## Preparation and Photocatalytic Performance of Spherical-like $\text{Bi}_4\text{Ti}_3\text{O}_{12}$ Composite

GAO Xiao-Ming, DAI Yuan, ZHANG Yu,  
WANG Zi-Hang, FU Feng

DOI:10.11862/CJIC.2017.046

*Chinese J. Inorg. Chem.*, **2017**,**33**:455-462



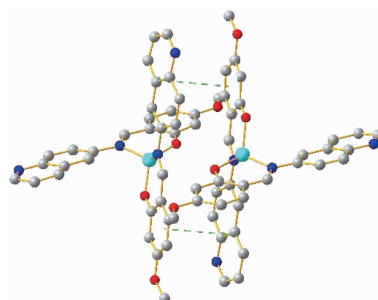
Spherical-like  $\text{Bi}_4\text{Ti}_3\text{O}_{12}$  composite was synthesized by hydrothermal method. With the assistance of self-assembly and anisotropic growth process, the surface energy will be further decreased, thus the spherical-like  $\text{Bi}_4\text{Ti}_3\text{O}_{12}$  composite becomes much more stable.  $\text{Bi}_4\text{Ti}_3\text{O}_{12}$  composite exhibited significantly photocatalytic activity under visible light irradiation towards degradation of AF than that of MO, MB, and the  $\cdot\text{OH}$  was main active radicals in photocatalytic degradation.

## Syntheses, Crystal Structures and Antibacterial Activities of Complexes with *N*-(6-Quinoly)salicylaldehyde Ligand

SHI Juan, LI Jiang, GE Hong-Guang

DOI:10.11862/CJIC.2017.050

*Chinese J. Inorg. Chem.*, **2017**,**33**:463-470



4-methoxy-6-amine quinoline Schiff base (L) coordinated with  $\text{Co}(\text{II})$ ,  $\text{Zn}(\text{II})$  and  $\text{Cu}(\text{II})$  to give complexes  $[\text{CoL}_2]$  (**1**),  $[\text{ZnL}_2]$  (**2**) and  $[\text{CuL}_2]$  (**3**). Complexes **1-3** had similar coordination mode, and the coordinate metal atom possessed a distorted tetrahedron. Complex **1** had an outstanding fungicidal activities, and can be used as antibacterial agent.

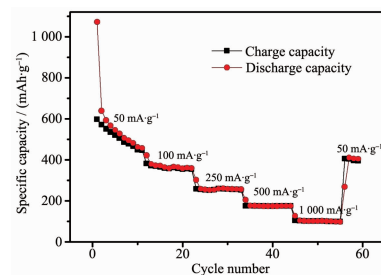


# Synthesis and Electrochemical Performances of Three-Dimensionally Ordered Macroporous $\text{Fe}_2\text{SiO}_4/\text{SiO}_2@\text{C}$ Nano-Glass-Ceramic Materials as an Anode for Lithium-Ion Batteries

SUN Ru, LI Dong-Lin, CHEN Guang-Qi, ZHANG Wei, FAN Xiao-Yong, GOU Lei, WANG Yan-Ru, CHENG Yi-Ni, ZHAO Zhen-Zhen

DOI:10.11862/CJIC.2017.058

*Chinese J. Inorg. Chem.*, **2017**,**33**:471-478



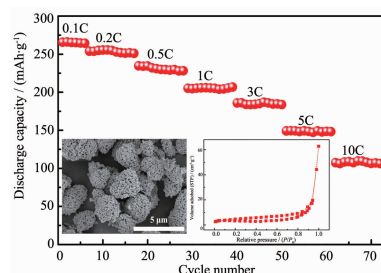
3DOM  $\text{Fe}_2\text{SiO}_4/\text{SiO}_2@\text{C}$  nano-glass-ceramic exhibits a highly reversible discharge capacity up to  $450 \text{ mAh} \cdot \text{g}^{-1}$  at a current density of  $50 \text{ mA} \cdot \text{g}^{-1}$ , and  $260 \text{ mAh} \cdot \text{g}^{-1}$  at  $250 \text{ mA} \cdot \text{g}^{-1}$  in the voltage range of 0.05~3.0 V, while 3DOM amorphous  $\text{SiO}_2@\text{C}$  composite with same porous structure only delivers  $15 \text{ mAh} \cdot \text{g}^{-1}$  at  $50 \text{ mA} \cdot \text{g}^{-1}$ .

# Preparation and Electrochemical Performance of Porous Micro-Nano Structure Layered Li-Rich $0.6\text{Li}_2\text{MnO}_3 \cdot 0.4\text{LiNi}_{0.5}\text{Mn}_{0.5}\text{O}_2$ Cathode for Lithium-Ion Batteries

ZHENG Zhuo, WU Zhen-Guo, XIANG Wei, YANG Xiu-Shan

DOI:10.11862/CJIC.2017.059

*Chinese J. Inorg. Chem.*, **2017**,**33**:479-486



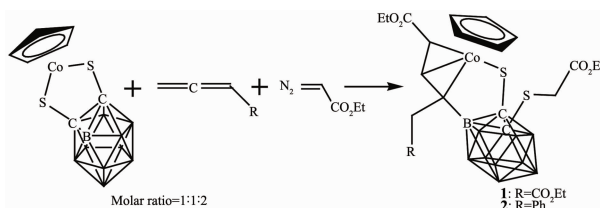
The porous micro-nano Li-rich  $0.6\text{Li}_2\text{MnO}_3 \cdot 0.4\text{LiNi}_{0.5}\text{Mn}_{0.5}\text{O}_2$  cathode has a well-ordered layered  $\alpha\text{-NaFeO}_2$  structure and high BET specific surface area ( $13 \text{ m}^2 \cdot \text{g}^{-1}$ ), which endows the significantly improved high rate performance ( $10\text{C}$ ,  $107 \text{ mAh} \cdot \text{g}^{-1}$ ) and cycling stability (94% of capacity retention at  $0.5\text{C}$  after 100 cycles).

# Reactivity of Half-Sandwich 16 Electron Compound $\text{CpCo}(\text{S}_2\text{C}_2\text{B}_{10}\text{H}_{10})$ with Ethyl Diazoacetate and Allenes(English)

LIU Gui-Feng, YAN Hong

DOI:10.11862/CJIC.2017.055

*Chinese J. Inorg. Chem.*, **2017**,**33**:487-492



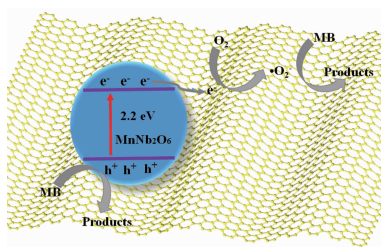
The three-component reactions of the 16e half-sandwich complex  $\text{CpCo}(\text{S}_2\text{C}_2\text{B}_{10}\text{H}_{10})$  (Cp: cyclopentadienyl) with ethyl diazoacetate (EDA) and terminal allenes at ambient temperature lead to compounds **1** and **2**. A plausible mechanism for the formation of **1** and **2** was proposed.

# Fabrication of RGO-MnNb<sub>2</sub>O<sub>6</sub> Photocatalyst with Enhanced Visible Light Efficiency in Photocatalytic Degradation of Methylene Blue (English)

GU Wei, YAN Ming, SUN Lin, SHI Wei-Dong

DOI:10.11862/CJIC.2017.054

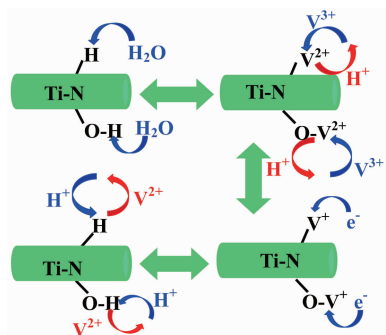
*Chinese J. Inorg. Chem.*, **2017**,**33**:493-500



The as-prepared RGO-MnNb<sub>2</sub>O<sub>6</sub> composites could significantly enhance photocatalytic activity for the degradation of methylene blue under visible light irradiation. Within 60 min, 78.2% of the methylene blue was removed by the optimum sample (3% RGO-MnNb<sub>2</sub>O<sub>6</sub>), which was about 2 times higher than that of the individual MnNb<sub>2</sub>O<sub>6</sub>.

Electrochemical Performance of  
Titanium Nitride Nanotubes as  
Negative Electrode in a Static  
Vanadium Battery Towards V(II)/V(III)  
Redox Couple (English)

ZHAO Feng-Ming, WEN Gang,  
KONG Li-Yao, CHU You-Qun, MA Chun-An



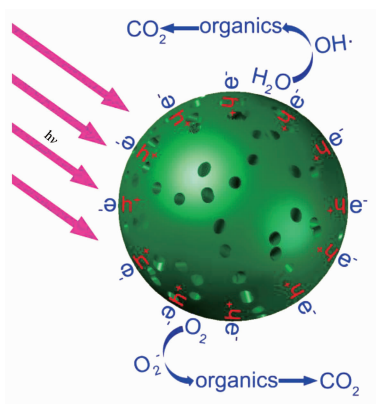
TiN NTs electrode provides large electrochemical surface area and more active center to improve the absorption of V(III), therefore the TiN NTs electrode exhibited excellent electrochemical activity towards V(II)/V(III) redox couple.

DOI:10.11862/CJIC.2017.053

*Chinese J. Inorg. Chem.*, **2017**,**33**:501-508

Synthesis and Photocatalytic  
Characterization of ZnO/BiOI  
Microspheres (English)

WANG Yuan-You, GONG Ai-Qing,  
YU Wen-Hua



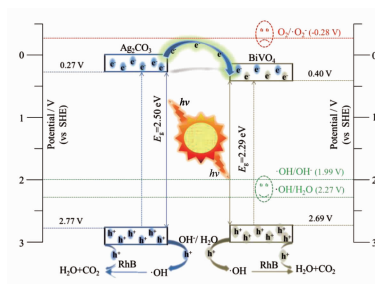
The porous ZnO/BiOI microspheres showed high photodegradation activities whether in RhB aqueous solution or in CH<sub>3</sub>CHO gaseous phase.

DOI:10.11862/CJIC.2017.061

*Chinese J. Inorg. Chem.*, **2017**,**33**:509-518

Preparation, Characterization and  
Photocatalytic Mechanism of  
Ag<sub>2</sub>CO<sub>3</sub>/BiVO<sub>4</sub> Composite Microsheets

LIU Ren-Yue, WU Zhen, BAI Yu,  
YU Chang-Lin, LI Jia-De, SHU Qing,  
YANG Kai



DOI:10.11862/CJIC.2017.062

*Chinese J. Inorg. Chem.*, **2017**,**33**:519-527